Geochemical Journal, Vol. 43, pp. 167 to 177, 2009

Microbial biomineralization of iron seepage water: Implication for the iron ores formation in intertidal zone of Zhoushan Archipelago, East China Sea

ZIJUN WU,[1] LINXI YUAN,[1] NAN JIA,[1] YUHONG WANG[2] and LIGUANG SUN[1]*

[1]Institute of Polar Environment, University of Science and Technology of China, Hefei, Anhui 230026, China
[2]National Institute of Health, Bethesda, Maryland 20892, U.S.A.

(*Received June 6, 2008; Accepted December 4, 2008*)

The biogeochemcical reactions responsible for fossilized minerals preservation in ancient geological conditions are very often debatable, because little is known about the *in situ* processes at geo-historical period. In the present study, we describe the formation of iron ores collected in the intertidal zone of the Zhujiajian Island, Zhoushan Archipelago in the East China Sea. Morphological, mineralogical and geochemical analyses were performed on the iron ores and the surrounding geological materials. The results show that the iron ores, composed of spherical ferrihydrite and fibrous aggregates of goethite, presented morphological characteristics reminiscent of bacterial activity. The biominerization process in the seepage system is believed to represent an analogue mechanism for the biogenic formation of iron ores. The degradation of the ancient wood layer provided humic substances which accelerated the leaching process of iron from the surrounding bedrock and soils. The abundant leaching iron not only provided the sufficient iron material source, but also created the ideal conditions for the survival of the iron-oxidizing bacteria. The presence of *Leptothrix*-like sheaths and *Gallionella*-like stalks in the present-day seepage environment promoted the oxidization of Fe^{2+} to Fe^{3+} and the rapid precipitation of bacteriogenic iron oxides (BIOS) on bacterial sheaths and stalks, allowing the preservation of the morphological characteristics of the bacteria. As time went by, the amorphous biomineralization product (ferrihydrite) can further transfer to more crystalline goethite and therefore be preserved in the ores permanently, representing as the imprints of bacterial activity during the formation of iron ores. The present findings should help elucidate the role of bacteria in the formation of biogenic iron ores in different environments during geo-historical context.

Keywords: ancient wood layer, seepage water, biomineralization, iron ores, intertidal zone

INTRODUCTION

Iron is the fourth most abundant element in the Earth's crust, which exists primarily as diversiform minerals in the divalent ferrous (Fe(II)) reduction or trivalent ferric (Fe(III)) oxidation states in natural environments (Ehrlich, 2002; Fortin and Langley, 2005). The formation of iron minerals is generally mediated by the activity of microorganisms, usually bacteria (Ferris *et al*., 1988; Ghiorse and Ehrlich, 1992; Mann *et al*., 1992; Akai *et al*., 1999; Brown *et al*., 1999; Tazaki, 2000; Ueshima and Tazaki, 2001; Tazaki, 2005), and the bacterial activity may leave some obvious imprints in the ancient minerals. Tazaki *et al*. (1992) found some fossilized remains of both filamentous and coccoid microoganisms in a stromatolitic grey chert with 2.0 Ga years old from Gunflint Iron Formation, and suggested iron mineral formation was associated with bacteria in the chert. Kamber *et al*. (2004) reported a stromatolite form Zambezi, and stated that the various layers of the stromatolite were created partly by the trapping of sediments by organisms, typically filamentous mats of cyanobacteria, algae, diatoms and bacteria (Lundgren and Dean, 1979; Reid and Browne, 1991). The Archean–Proterozoic is characterized by large iron deposits known as banded iron formations (BIF), and the occurrence of BIF demonstrates the important role of bacterial biomineralization in the early stages of Earth history (Holm, 1987; Nealson and Myers, 1990; Konhauser *et al*., 2002). In addition, the bacterial contribution to the formation of small sedimentary iron ore deposits, such as bog iron ore or lacustrine Fe/Mn ore is also considered likely (Pontus, 1955; Crerar *et al*., 1979; Dubinina, 1981).

The role of bacteria in mineral formation results from the reactivity of the bacterial cell wall and extracellular polymers, which contain functional groups that can facilitate the sorption of metal ions, such as Fe^{2+} and Fe^{3+} onto their surface. These metal ions may then act as nucleation sites for the deposition of further minerals from solution, e.g., Bacteriogenic iron oxides (BIOS) (Beveridge and Fyfe, 1985; Fortin and Beveridge, 1997; Fortin *et al*., 1998; Brown *et al*., 1999; Ueshima and

*Corresponding author (e-mail: slg@ustc.edu.cn)

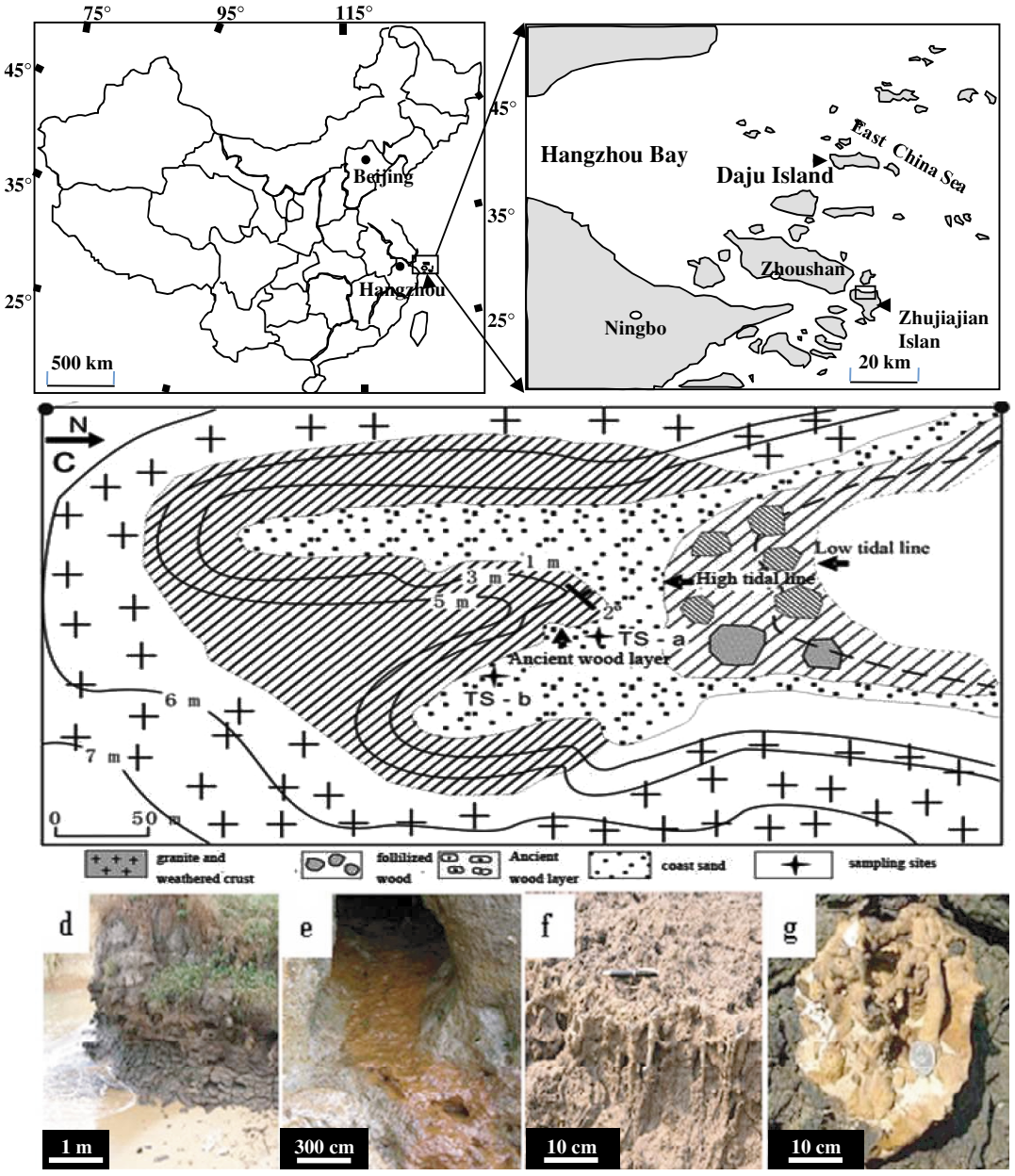

Fig. 1. Maps showing the geological background of sampling sites (a and b, geographic position of sampling sites; c, geological profile of sampling sites; d, ancient-wood layer; e, brownish orange seepage water; f and g, iron ores).

Tazaki, 2001; Anderson and Pedersen, 2003; Chan *et al*., 2004). BIOS are composite materials that consist of intact and partly degraded remains of bacterial cells intermixed with variable amounts of poorly ordered hydrous ferric oxide (HFO) minerals (Ferris *et al*., 1999, 2000; Anderson and Pedersen, 2003). And BIOS are common in groundwater environment. They are formed when chemical or bacterial oxidation of Fe^{2+} gives rise to Fe^{3+}, which then undergoes hydrolysis to precipitate in association with bacterial cells. Because of their broad distribution and reactive surface properties, BIOS are believed to play an important role in regulating the fate and behavior of dissolved iron ions (Ferris, 2005).

Though many studies have documented the specific characteristics (i.e., the mineral type, orientation of crystallographic axes, microarchitectures and isotope composition) that could be ascribed to a biological origin (Lowenstam, 1981; McKay *et al*., 1996; Tazaki *et al*.,

1992; Beard *et al*., 1999; Croal *et al*., 2004), it is still scarcity of direct evidence for discriminate between true biogenic minerals and those formed as resulted of abiotic reactions in natural environments. Therefore, microbial iron precipitation requires further evaluation.

In this study, we describe the morphological, geochemical and mineralogical characteristics of iron ore specimens from the intertidal zone of Zhoushan Archipelago, East China Sea, and microbial biomineralization occurring in the present-day iron seepage water there. The objective of this study is to evaluate the biogenic nature of the iron ores and to discuss the iron biomineralization mechanisms of the iron ores, based on the comparing the microbial biomineralization characteristics of iron seepage water with biogeochemical characteristics of the ancient iron ores. This is expected to provide some insights into the formation of fossilized iron ore deposits in geohistorical context.

Materials and Methods

Background description and samples collection

In 1996, an ancient wood layer and iron ores were discovered in the intertidal zone of Zhujiajian Island, Zhoushan Archipelago in East China Sea (Figs. 1a, b, c, and d). The ancient wood layer occurring along the sea coast is about 3.3 m thick, containing a large number of ancient tree stems with a diameter ranging from 1 to 85 cm. The largest stem is 5.6 m long and was identified as sweetgum (*Liquidambar formosana Hance*) of the witchazel family (*Hamamelidaceae*) (Sun *et al*., 2000). By AMS^{14}C dating method, the largest ancient wood (sweetgum) was dated as 5600 ± 40 cal. yr B.P. Under the ancient wood, black peat layer and granitic bedrock were observed. Furthermore, several caves occurred near the ancient wood layer and the seepage water emanating from the rock wall produced brownish orange iron mud of various thicknesses (Fig. 1e). The seepage water flow is slow (<1 m/s) and moves towards the intertidal zone. There are also some concretions in the beach mud and many iron ores near the ancient wood layer (Figs. 1f and g), which appear to be strongly influenced by the seepage water. The iron ores shaped like cemented tube or plant root have a brownish yellow color and generally, the each tube or plant root has 2 to 3 cm in diameter and 5 to 10 cm in length. They are rigid, but fragile with a density about 2.67 g/cm^3 (Yuan *et al*., 2008).

During the 1998 field work, iron ores, fresh bedrock (granite), weathering bedrock profiles and beach sediments (surface) samples were collected in the intertidal zone of Zhujiajian Island, Zhoushan Archipelago, East China Sea. And then in September 2006, water samples were collected at two sites in the seepage area. The seepage water samples were stored in polyethylene bottles labelled as TS-a and TS-b (Fig. 1c), respectively. *In situ* temperature (*T*), dissolved oxygen (DO), pH and oxidation reduction potential (ORP) measurements were performed in the seepage area, using an Orion 5-Star Portable pH/ORP/DO/Conductivity Multimeter. And the seepage water has a temperature of 23–25°C, pH of 6–7, Eh of 170–250 mV and dissolved oxygen (DO) of 1.5–5 mg/L (Table 2). The fresh bacteriogenic iron oxides (BIOS) were also recovered at each seepage site using sterile plastic spatulas. The samples were placed directly into 100 ml polypropylene tube, and sub samples were fixed in 10 ml centrifuge tubes with 2% (v/v) gluteraldehyde mixed with the seepage water. All of the sample tubes were sealed with screw caps, and stored at 4°C until their analysis.

Chemical and mineralogical analyses

Each subsample of the iron ores, fresh bedrock, weathering bedrock profile and beach sediments was first air-dried, powdered and sieved through a 100 mesh. 0.1–0.5 g of each powder sample was then precisely weighted and digested with multi-acid (1 ml HF + 1.5 ml HCl + 0.5 ml HNO_3) in a polytetrafluoroe thylene (PTFE) crucible with electric heating. The major elements/oxides for digested samples were determined by Atomscan Advantage Inductively Coupled Plasma Atomic Emission Spectrometer (ICP-AES). For quality control purpose, certified reference materials (CRMs, supplied by National Research Center for CRM's of China, Beijing) were used as internal standards in proportion of 10% of total analyzed samples. The analytical values for the major elements are within 5% of those of the certified ones.

SO_4^{2-} and Cl^- concentrations in the seepage water were determined by an ion chromatography (DX-600, America) and Na^+, K^+, Mg^{2+}, Ca^{2+}, SiO_4^{2-}, total Mn and Fe were analyzed by ICP-AES (Atomscan Advantage, America). Fe^{2+} was measured by colorimetric method using ultraviolet visible spectrophotometry (UVS) (UV-VIS-8500, China).

Powder X-ray diffraction was used to determine the mineralogy and crystallinity of the iron ore samples by D/MAX-RA diffractometer (Rigaku, Japan). The samples were dried at 60°C and then analyzed with Cu Kα radiation from 3° to 90°, with a step size of 0.020 and a rate of 0.85 s/step.

Microscopic analyses

Scanning electron microscope (SEM) observation For SEM observation, approximately 1 ml fresh BIOS from seepage water fixed with 2% (v/v) gluteraldehyde was washed three times with ultra-pure water (UPW) by centrifugation at 3200 × g for 5 min. The washed wet samples were then re-suspended in 250 ml of UPW and vacuum filtered onto white uncleopore track-etch 0.2 μm

Table 1. Elemental composition of the iron ores and the related environmental materials

Dry wt. %	Iron ores (*n = 5)	Beach sediment	Fresh BIOS	Weathering bedrock profile		Fresh bedrock (granite)
				Red soil (*n = 4)	White soil (*n = 4)	
SiO_2	36.03	61.26	37.28	66.77	70.98	77.53
Al_2O_3	12.33	9.71	10.40	15.51	15.65	12.02
TiO_2	0.12	0.44	0.35	0.70	0.79	0.12
Fe_2O_3	49.29	2.13	41.54	5.97	1.65	0.91
MnO	0.35	0.034	0.51	0.03	0.02	0.095
K_2O	1.27	2.01	1.52	2.87	3.05	4.77
Na_2O	0.07	1.73	1.08	1.28	1.20	3.88
CaO	0.08	0.70	nm	nm	nm	nm
MgO	1.75	0.82	nm	0.52	0.50	nm

Note: "nm" not measured; "" number of the measured samples.*

pore-size filters. The filter paper was subsequently dehydrated using graded series of ethanol solutions (10, 25, 50, 80, 100% v/v). Following dehydration, filters were cut and mounted on to Al stubs using carbon tape, and then were Au-coated. Examination of the samples was done using a X'PERT PRO SEM (Quanta 200) at an accelerating voltage of 15 kV.

Transmission electron microscope (TEM) observation and micro-area analysis TEM and high-resolution TEM (HRTEM) were used to observe the micro-morphological characteristics of fresh BIOS and iron ores, respectively. Whole mounts were prepared by dropping gently crushed samples onto Formvar-carbon-coated 200-mesh copper grids. Excess sample was then carefully removed with a filter paper and the grids were air-dried for HRTEM analysis on iron ores samples. For TEM analysis, the fresh BIOS samples pre-fixed with 2% glutaraldehyde were dehydrated in a series of ethanol solutions (25, 50, 75, and 100% v/v) for 15 min each, and then infiltrated with 50% (v/v) epoxy resin (TAAB) and ethanol for 1 hour. Subsequently, the processed samples were mixed with pure epoxy resin for another hour prior to be polymerized for 8–10 hours at 60°C. Ultrathin sections (0.2 μm) were cut with a diamond knife and deposited onto Formvar-carbon-coated 200-mesh copper grids. The sections were then stained with uranyl acetate to enhance the electron contrast of the biological material. Specimens were examined with a JEOL-2010 TEM/HRTEM (Japan) equipped with a Link Analytical energy dispersive X-ray spectroscopy (EDS) system. The chemical composition of mineral precipitates on the surface of the bacteria was analyzed by EDS at 100 kV for 100 s live time with a beam current of 0.1 μA. Identification of the precipitates on the individual bacterial surfaces was accomplished by selected area electron diffraction (SAED) at an accelerating voltage of 100 kV.

RESULTS

Chemical composition of the iron ores and surrounding geological material

Table 1 lists the elemental composition of the iron ores and the surrounding geological samples. The major elemental compositions are Fe_2O_3, SiO_2, and Al_2O_3 for the iron ores, and the mean content of Fe_2O_3 is 49.29 wt. %, SiO_2 is 36.03 wt. %, and Al_2O_3 is 12.33 wt. % (n = 5), respectively. Compared with the fresh bedrock, the oxides of Fe in iron ore are concentrated by a factor of 8.2–54.1, and the Si oxides content are about half of that in the fresh bedrock. In addition, soluble elements (such as K_2O, Na_2O) are much lower in the iron ores than that in the fresh bedrock, especially for Na_2O. However, the differences in major oxides content between the iron ores and the fresh BIOS are not significant.

In addition, the observation in the field on the profile of the wood layer shows significant signs of weathering, as indicated by the red soil at the top and the white soil at the bottom (Yuan *et al*., 2008). The red soil samples (n = 4) have a total Fe concentration ranging from 40.6 to 98.3 mg/g (with an average of 59.7 ± 26.1 mg/g). On the other hand, the white soil samples (n = 4) have a lower total Fe content (i.e., 14.6 to 18.3 mg/g with an average of 16.5 ± 2.6 mg/g), suggesting that iron cycling within the weathering bedrock profile likely be affected by the ancient wood layers. Meanwhile, the measured pH value of peat layer in the ancient wood layer is about 3.0.

Morphology and mineral composition of the iron ores

Optical observations of the iron ore specimens showed that transparent minerals represented 70% of the entire mineral assemblage and corresponded to quartz, feldspar, and mica. The remainder opaque minerals showed a cryptocrystalline aggregation of iron minerals. The quartz

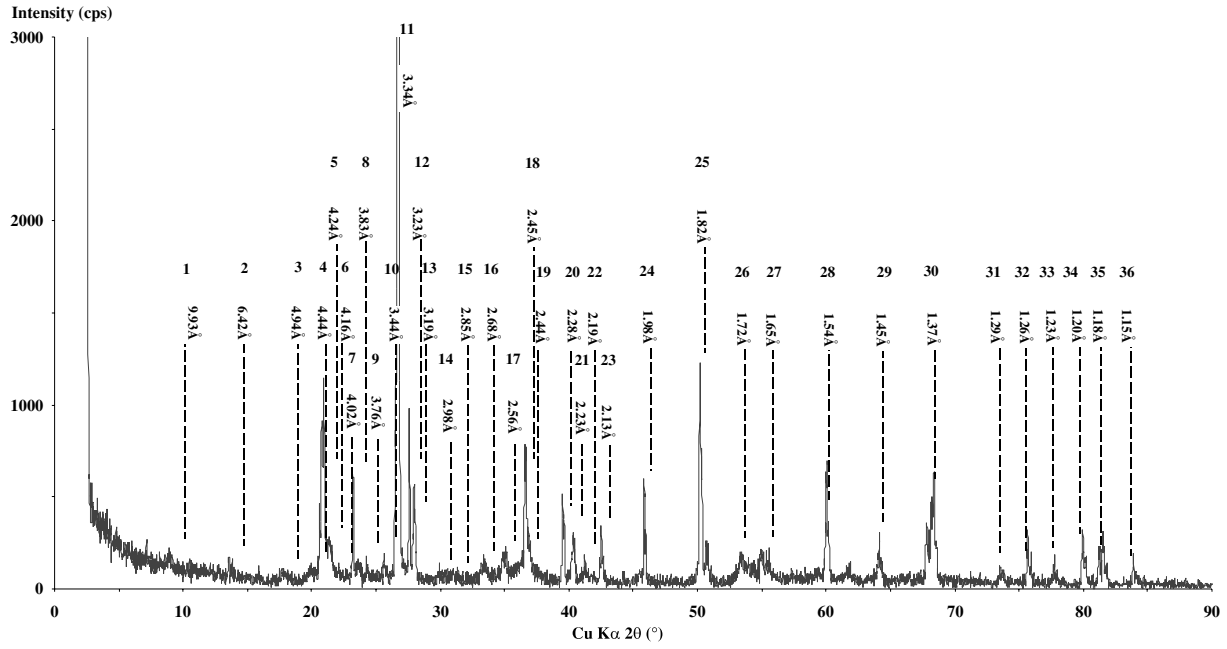

Fig. 2. The XRD patterns for the sample of iron ores. Albite (A): 2, 7, 8, 9, 10, 12, 13, 14, 15, 17, 19; Muscovite (M): 1, 4, 10, 11, 13, 14, 15, 17, 18, 23; Goethite (α-FeOOH) (G): 3, 6, 16, 18, 22, 26; Quartz (Q): 5, 18, 20, 21, 23, 24, 25, 27, 28, 29, 30, 31, 32, 33, 34, 35, 36.

particles showed sharp edges and corners which are indicative of short distance transport. X-ray diffraction (XRD) analysis confirmed the iron ore samples mainly contained Quartz (Q), Albite (A), Muscovite (M), and Goethite (α-FeOOH) (G) (Fig. 2). These results indicate that the minerals of iron ores are derived from the weathering of the local acidic bedrock (granite).

HRTEM-EDS analyses of the iron ores show the presence of two different particulate textures. They are fibrous particles with a diameter of 5–30 nm and a length up to 1 μm (Figs. 3a and b) and assemblages of spherical materials with a diameter of 20–200 nm (Fig. 3e). The fibrous materials mainly contained Fe K*d* (Fig. 3d), and were characterized by SEAD with d-spacing values of 2.58 Å, 2.45 Å and 2.19 Å, corresponding to goethite (Fig. 3c). However, the spherical materials also mainly contained Fe K*d*, but SAED revealed that it was poorly crystalline 2-line ferrihydrite (Fig. 3g). More importantly, TEM observations of iron ores confirm the presence of some fossilized remnants with bacillus, which may be represented as biomineralizated bacteria, with a diameter of 100–200 nm and a length up to 1 μm. The bacillus were coated with semi-granular materials and bundles of minerals in more details (Figs. 3h and i).

Table 2. The geochemical composition of seepage water

	TS-a	TS-b
T (°C)	23.40	25.00
pH	6.00	6.99
Eh (mV)	248.80	171.10
DO (mg/L)	5.19	1.75
Cl^- (μmol/L)	740.00	689.00
SO_4^{2-} (μmol/L)	1270.00	860.00
NO_3^- (μmol/L)	1.90	6.10
Na^+ (μmol/L)	523.50	79.50
K^+ (μmol/L)	202.00	111.00
Mg^{2+} (μmol/L)	533.60	99.30
Ca^{2+} (μmol/L)	720.30	86.20
Mn^{2+} (μmol/L)	25.54	nd
Al^{3+} (μmol/L)	20.08	1.08
Si–SiO_3^{2-} (μmol/L)	94.95	34.26
Fe^{2+} (μmol/L)	198.80	23.80
Total Fe (μmol/L)	241.60	26.50

Note: "nd" not detected.

Chemical and microbial characteristics of the present-day iron seepage system

The physico-chemical characteristics of the seepage water samples (TS-a and TS-b) are shown in Table 2. The seepage water is characterized by a nearly neutral pH (6–7), low oxygen content (1.75–5.19 mg/L) and high levels of ferrous iron (23.8–198.8 μmol/L). The other main ions

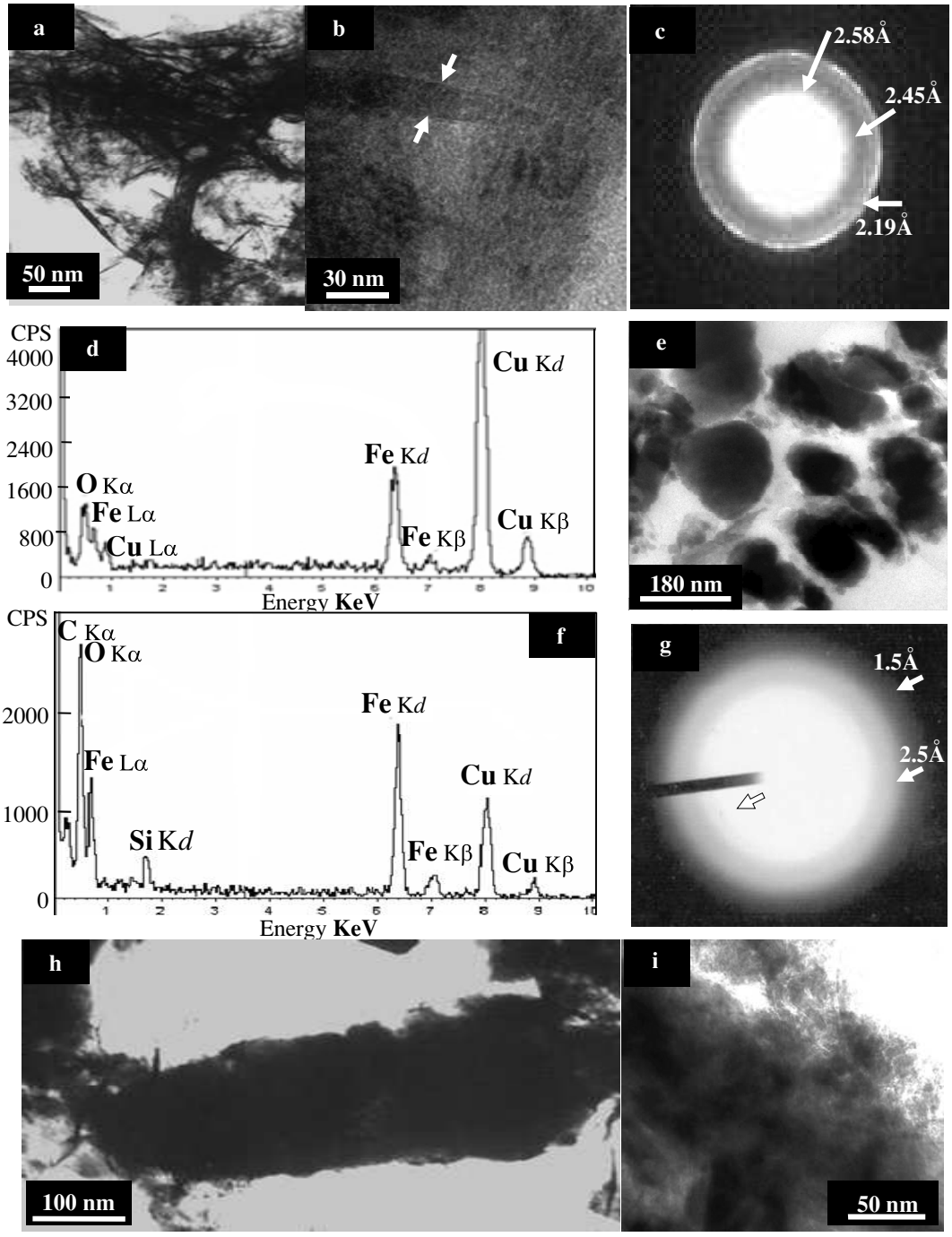

Fig. 3. TEM images showing the microstructures of the iron ores containing fibrous material (a, b), (c) the selected area electron diffraction (SAED) spectrum of the fibrous material, which was determined to be goethite, (d) the energy dispersive spectrum (EDS) of fibrous material mainly contained Fe, (e) showing some spherical material in the iron ores, (f) the energy dispersive spectrum (EDS) of spherical material mainly contained Fe, and it was determined as poorly crystalline 2-line ferrihydrite by SAED (g), some remnant structure of mineralized dead bacteria was observed in the iron ores (h, i).

are Cl^-, SO_4^{2-}, K^+, Na^+ and Ca^{2+}. These results indicate that the seepage water is a mixture of fresh meteoric water, modern seawater (pH ≈ 8) and underground water in contact with the surrounding bedrock.

The iron oxide precipitates in the seepage area contained heterogeneous mixture of fine-grained particles and microbial cells, which were usually called bacteriogenic iron oxides (BIOS) (Figs. 4a, b, and c). The tube frag-

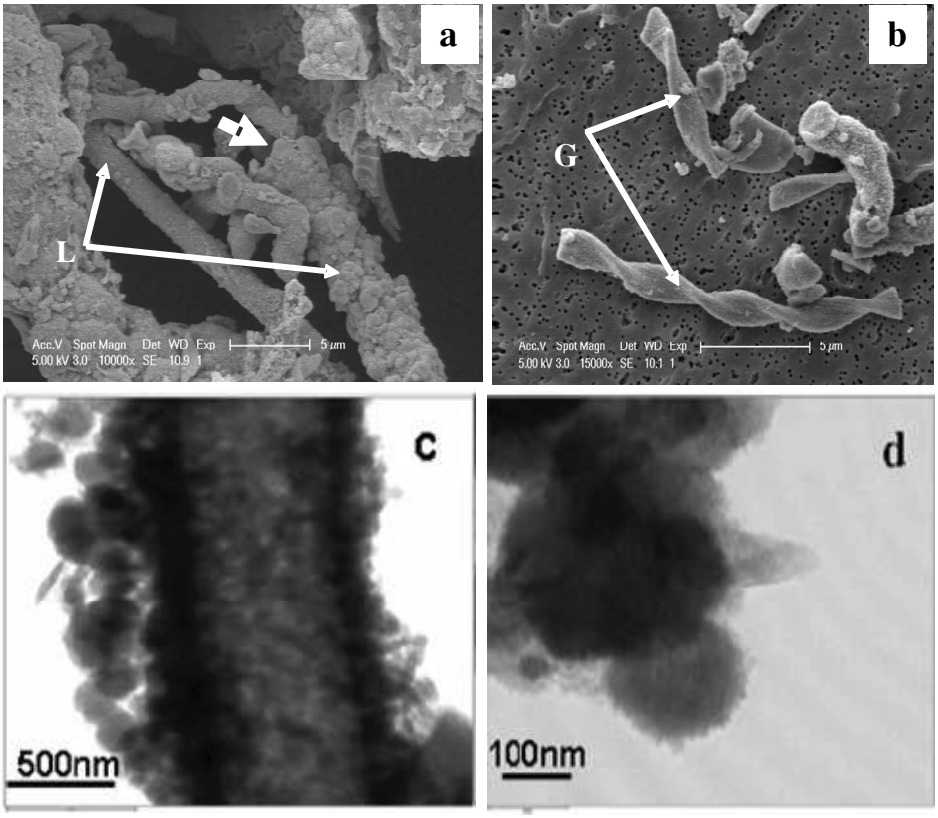

Fig. 4. The SEM and HRTEM photos of iron mud in seepage system (SEM images of mineralized bacterial surfaces resembling the sheath of Leptothrix-like (L) and the stalk of Gallionella-like (G) (a, b), HRTEM showing the aggregates of iron oxides encrusted on the surface of bacterial sheaths (c, d).

ment shown in Fig. 4a is characteristic of *Leptothrix*-like sheaths (Emerson and Revsbech, 1994), while the distinctive helical structure in Fig. 4b is representative of the metabolic materials from *Gallionella*-like stalk (Hallbeck and Pederson, 1991; Hallberg and Ferris, 2004). These two bacteria are known as neutrophilic iron-oxidizing bacteria (Kennedy *et al.*, 2003; James and Ferris, 2004; Fortin and Langley, 2005). Fine-grained mineral precipitates were also commonly observed on the bacterial sheaths and stalks (Fig. 4c). Their size varied between 20 and 500 nm (Fig. 4d). TEM observations of thin sections showed that the mineral precipitates often occurred in the close vicinity of the bacterial cell walls and bacterial exopolymers (Figs. 5a and b). In some cases, the bacterial cell wall appeared to be partially preserved by the minerals, but the complete replacement of the cells was more common, which produced particles with no apparent texture (Figs. 5c and d). TEM-EDS analysis revealed that the fine-grained minerals in association with the bacteria were Fe-rich plus some Mn (Fig. 5e). The mineralogy of the particles was confirmed by TEM-SAED analysis which indicated the presence of 2-line ferrihydrite, with d-spacing values of 2.5 Å and 1.5 Å (Fig. 5f) (Kennedy *et al.*, 2003, 2004).

Discussion

Iron origin for formation of iron ores

It is shown in Table 1 that the change of elemental contents of weathering bedrock profile is significantly affected by the buried ancient wood layer. It is known that ancient wood layers could produce enough organic acids during their buried process, which can accelerate the weathering process of the nearby granite bedrock with the chemical or biological reaction (Hama *et al.*, 2001; Coombs *et al.*, 2008). Based on the investigation in the field, a thick peat layer was buried under the ancient wood layer and its measured pH value is about 3.0. As a result, the iron minerals present in the granite, such as hornblende and biotite, were reduced by humic substances (Weber, 1988; Tipping and Hurley, 1992; Schmitt *et al.*, 2002; Kaczorek and Sommer, 2003), especially the humic acids from the ancient wood layers. In this case, Fe^{2+} ions were leached out of the bedrock and transported via

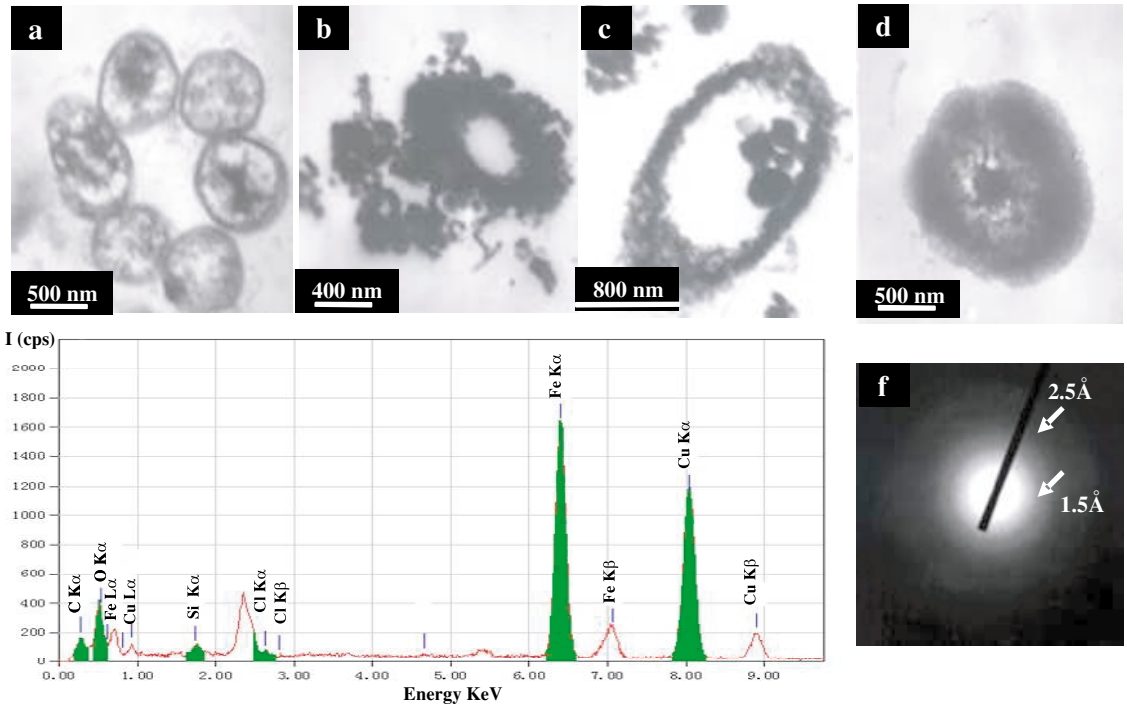

Fig. 5. TEM thin section of the iron seepage deposit showing (a) iron oxides occurring in the close vicinity of bacterial cell walls, (b) bacterial exopolymers, (c) biomineralization near the bacterial cell walls, (d) bacterial structures completely replaced by dense amorphous materials, (e) TEM-EDS analysis revealing that mineral precipitation on the surface of bacteria is mainly composed of Fe (Cu is from the supporting grid), and (f) TEM-SAED analysis of the mineralized bacterial surface.

groundwater into the sandy beach or in the intertidal zone (Weber, 1988; Warren and Haack, 2001), providing sufficient material source for formation of iron minerals in favour biogeochemical condition.

Due to the different mobility of the elements in surrounding environments, it results in the differences of elemental contents in the weathering bedrock profile, seepage water, fresh BIOS, beach sediments and iron ores (Tables 1 and 2). Especially, the Al and Si belong to immobile major elements, which can be easily preserved in the remnant product of weathering. On the contrary, the Mg, Ca, K and Na are characterized of high mobility, and they can be easily leached out from the bedrock or soils to the beach sediments or seawater (Liu *et al*., 2005). Furthermore, the presence of anatase (TiO_2) (Table 1) is also indicative of strong weathering, resulting in low content of soluble elements such as Ca, Na and Mg in the iron ores.

Biomineralization in the present-day seepage water system

In the seepage water systems, pronounced redox and oxygen gradients likely developed during the mixing of meteoric water, seawater and underground water, as a result of tide dynamics. Such gradients provide ideal chemical conditions for specific lithoautrophic bacteria (Petersen, 1997; Ferris *et al*., 1999), namely iron-oxidizing bacteria (i.e., *L. ochracea* and *G. ferruginea*). The bacterial forms observed in the iron oxide deposits from the seepage area (Fig. 4) share a striking similarity with *L. ochracea* and *G. ferruginea*, but their identification cannot be ascertained based solely on their morphology. However, the cells were found in close association with iron oxides (Figs. 4 and 5), which strongly suggests that they are indeed iron-oxidizing bacteria. The precipitation of iron oxides on the stalks of *G. ferruginea* and sheaths of *L. ochracea* is a well-documented phenomenon interpreted as a direct consequence of the metabolic oxidation of ferrous iron by bacteria (Ferris *et al*., 1999; Ferris, 2005; Kennedy *et al*., 2003). Some studies have indicated that iron-oxidizing bacteria accounts for at least 50% and up to 90% of Fe^{2+} oxidation in neutral pH waters, particularly under diffusion limiting conditions at the aerobic-anaerobic interface (Emerson and Revsbech, 1994; James and Ferris, 2004; Sobolev and Roden, 2004). The close physical association observed by SEM and TEM between the bacteria and iron oxides in the seepage system indicates that individual bacterial sheaths and stalks

behaved as geochemically reactive solids in the seepage water environment. In other words, the accretion of iron oxide precipitates onto bacteria indicates that bacteria played two causal roles in the precipitation of iron oxides. They firstly increased the iron-oxidation rate over the rate of inorganic oxidation, and also lowered the degree of super saturation required for iron oxide precipitation by behaving as heterogeneous nucleation sites (Fortin *et al*., 1998; Anderson and Pedersen, 2003; Chatellier *et al*., 2003; Kennedy *et al*., 2003; Fortin and Langley, 2005). The mineralogy of the iron oxides in the seepage system is also in agreement with other studies that consistently documented 2-line ferrihydrite as a product of biomineralization (Kasama and Murakami, 2001; Kennedy *et al*., 2003). This poorly ordered mineral may however transform to more crystalline iron minerals (i.e., goethite and hematite) after the bacteria's death and become microfossils (Tazaki *et al*., 1992; Dai *et al*., 2004; Kennedy *et al*., 2004).

Present-day seepage systems: an analogue for biologically mediated formation of iron ores?

Many studies have suggested that minerals forming as a result of microbial activity could present special structures, such as spherical aggregates of different sizes (Tazaki *et al*., 1992; Fortin *et al*., 1998; Akai *et al*., 1999; Tazaki, 2000, 2005; Williams *et al*., 2005). The TEM-EDS-SAED pictures of the iron ores showed many fibrous or spherical aggregates of goethite or ferrihydrite, respectively (Figs. 3a, b, and e), and these aggregates are similar in shape to those from bacterial mineralization. In addition, the presence of some fossilized remnants with bacillus in the iron ores (Figs. 3h and i) strongly suggested that microbial activity might have been involved in the formation of the iron ores.

The products of biomineralization in the seepage water system can further provide an insight into the potential processes responsible for the iron ores formation. In the present-day iron seepage environments, the physical and geochemical conditions support the presence of active iron-oxidizing bacteria. These bacteria accelerate the rate of Fe^{2+} oxidation and promote the formation of BIOS. Precipitation of BIOS on bacterial sheaths and stalks allows the preservation of the morphological characteristics of the bacteria, due to the relatively inert nature of the iron oxides in comparison to the organic constituents of the microbial cell. Furthermore, the preservation of mineralized bacterial cells can also be enhanced by the binding of metals, which inhibit cell lysis and contribute to bacterial preservation (Ferris *et al*., 1988; Kennedy *et al*., 2003). As a result, BIOS and the totally mineralized cells represent potential microfossils, which can slowly transform from amorphous composition to more crystalline iron oxides (Kennedy *et al*., 2003), such as those observed in the iron ores, i.e., goethite (Figs. 3a, b, e, h, and i).

Biomineralization processes, in general, can be classified into two categories: biologically controlled mineralization (BCM) and biologically induced mineralization (BIM) (Lowenstam, 1981). BIM processes are characterized by the precipitation on and within cells and the mineral grains have no controlled morphology and size distribution (Akai *et al*., 1999). The results described above suggest that the iron ores might have resulted from BIM processes. The iron-oxidizing bacteria use Fe^{2+}, O_2 or CO_2 from the water and the poorly-ordered iron oxides precipitate inside and outside the bacteria, especially in or on the cell wall and sheaths of bacteria (Dai *et al*., 2004).

CONCLUSIONS

The iron ores which were discovered in the intertidal zone of Zhoushan Archipelago, East China Sea, were mainly composed of spherical 2-line ferrihydrite and fibrous aggregates of goethite. After comparing with fresh BIOS from the seepage system in the study site, iron-oxidizing bacteria, such as *Leptothrix* and *Gallionella*, were very likely involved in the formation of the iron ores. Those iron minerals present in the coast bedrock (granite), such as hornblende and biotite, were reduced by humic substance from the ancient wood layers in the study site, and therefore provided abundant iron source for the iron-oxidizing bacteria and the formation of the iron ores. Consequently, Fe^{2+} ions were leached out of the bedrock and transported via groundwater to the sandy beach or the intertidal zone. This was followed by the precipitation of iron minerals around the ancient wood, where low oxygen, high Fe^{2+} and nearly neutral pH conditions favour the presence of iron-oxidizing bacteria. These bacteria can accelerate the iron oxidation rate and the accretion of iron minerals on bacterial sheaths or stalks, allowing the preservation of the morphological characteristics of the bacteria. As time went by, these amorphous BIOS can further transfer to more crystalline goethite and therefore be preserved permanently, representing as the imprints of bacterial activity during the formation of iron ores. The above findings should provide some insights into fossilized iron ores formation in a geo-historical context.

Acknowledgments—The authors would like to thank Dr. D. Fortin for valuable suggestions in preparing this manuscript. We also thank Dr. Tazaki and an anonymous reviewer for their valuable critical comments in improving manuscript. We also acknowledge Dr. Watanabe, associate editor of *Geochemical Journal* for his effort on dealing with our manuscript. This research was financed by the Projects of the Knowledge Innovation of CAS (Grant No. KZCX3-SW-151) and the Chinese Postdoctoral Science Foundation (Grant No. 20060400723).

References

Akai, J., Akai, K., Ito, M., Nakano, S., Maki, Y. and Sasagawa, I. (1999) Biologically induced iron ore at Gunma iron mine, Japan. *Am. Mineral.* **84**, 171–182.

Anderson, C. R. and Pedersen, K. (2003) *In situ* growth of Gallionella biofilms and partitioning of lanthanides and actinides between biological material and ferric oxyhydroxides. *Geobiol. J.* **1**(2), 169–178.

Beard, B. L., Johnson, C. M., Cox, L., Sun, H. and Nealson, K. H. (1999) Iron isotope biosignatures. *Science* **285**, 1889–1892.

Beveridge, T. J. and Fyfe, W. S. (1985) Metal fixation by bacterial cell walls. *Can. J. Earth Sci.* **22**, 1893–1898.

Brown, D. A., Sherriff, B. L., Sawickl, J. A. and Sparling, R. (1999) Precipitation of iron minerals by a natural microbial consortium. *Geochim. Cosmochim. Acta* **63**, 2163–2169.

Chan, C. S., De Stasio, G., Welch, S. A., Girasole, M., Frazer, B. H., Nesterova, M. V., Fakra, S. and Banfield, J. F. (2004) Microbial polysaccharides template assembly of nanocrystal fibers. *Science* **303**, 1565–1658.

Chatellier, X., Ravenel, C., Blanco, C., Fortin, D., West, M., Leppard, G. and Ferris, G. (2003) How bacteria can induce the formation of nanoparticles of Fe-oxides in their vicinity. *Geochim. Cosmochim. Acta* **67**, A58, 83–98.

Coombs, P., West, J. M., Wagner, D., Turner, G., Noy, D. J., Milodowski, A. E., Lacinska, A., Harrison, H. and Bateman, K. (2008) Influence of biofilms on transports of fluids in subsurface granitic environments—some mineralogical and petrographical observations of materials from column experiments. *Mineral. Mag.* **72**(1), 393–397.

Crerar, D. A., Knox, G. W. and Means, J. L. (1979) Biogeochemistry of bog iron in the New Jersey Pine Barrens. *Chem. Geol.* **24**, 111–135.

Croal, L. R., Johnson, C. M., Beard, B. L. and Newman, D. K. (2004) Iron isotope fractionation by Fe(II)-oxidizing photoautotrophic bacteria. *Geochim. Cosmochim. Acta* **68**, 1227–1242.

Dai, Y. D., Song, H. M. and Shen, J. Y. (2004) Fossil bacteria in Xuanlong iron ore deposits of Hebei Province. *Science in China Ser. D: Earth Sciences* **47**, 347–356.

Dubinina, G. A. (1981) The role of microorganisms in the formation of the recent iron-manganese lacustrine ores. *Geology and Geochemistry of Manganese III* (Grasselly, G., ed.), 305–326, Hungarian Academy of Science, Budapest, Hungary.

Ehrlich, H. L. (2002) Geomicrobiology of iron. *Geomicrobiology* (Ehrlich, H. L., ed.), 345–428, Marcel Dekker, Inc., New York, U.S.A.

Emerson, D. and Revsbech, N. P. (1994) Investigation of an ironoxidizing microbial mat community located near Aarhus, Denmark: field studies. *Appl. Environ. Microbiol.* **60**, 4020–4031.

Ferris, F. G. (2005) Biogeochemical properties of bacteriogenic iron oxides. *Geomicrobiol. J.* **22**, 79–85.

Ferris, F. G., Fyfe, W. S. and Beveridge, T. J. (1988) Metallic ion binding by Bacillus Subtilis: Implications for the fossilization of microorganisms. *Geology* **16**, 149–152.

Ferris, F. G., Konhauser, K. O., Lyven, B. and Pedersen, K. (1999) Accumulation of metals by bacteriogenic iron oxides in a subterranean environment. *Geomicrobiol. J.* **16**, 181–192.

Ferris, F. G., Hallberg, R. O., Lyven, B. and Pedersen, K. (2000) Retention of strontium, cesium, lead and uranium by bacterial iron oxides from a subterranean environment. *Appl. Geochem.* **15**, 1035–1042.

Fortin, D. and Beveridge, T. J. (1997) Microbial sulfate reduction within mine tailings: formation of diagenetic Fe-sulfides. *Geomicrobiol. J.* **14**, 1–21.

Fortin, D. and Langley, S. (2005) Formation and occurrence of biogenic iron-rich minerals. *Earth Sci. Rev.* **72**, 1–19.

Fortin, D., Ferris, F. G. and Scott, S. D. (1998) Formation of Fe-silicates and Fe-oxides on bacterial surfaces in samples collected near hydrothermal vents on the Southern Explorer Ridge in the northeast Pacific Ocean. *Am. Mineral.* **83**, 1399–1408.

Ghiorse, W. C. and Ehrlich, H. L. (1992) Microbial biomineralization of iron and manganese. *Biomineralization: Processes of Iron and Manganese* (Skinner, H. C. W. and Fitzpatrick, R. W., eds.), 75–99, CatenaVerlag, Cremlingen, Germany.

Hallbeck, L. and Pedersen, K. (1991) Autotrophic and mixotrophic growth of Gallionella ferruginea. *J. Gen. Microbiol.* **137**, 2657–2661.

Hallberg, R. and Ferris, F. G. (2004) Biomineralization by Gallionella. *Geomicrobiol. J.* **21**, 325–330.

Hama, K., Bateman, K., Coombs, P., Hards, V. L., Milodowski, A. E., West, J. M., Wetton, P. D., Yoshida, H. and Aoki, K. (2001) Influence of bacteria on rock-water interaction and clay mineral formation in subsurface granitic environments. *Clay Minerals* **36**, 599–613.

Holm, N. G. (1987) Possible biological origin of banded iron-formations from hydrothermal solutions. *Orig. Life.* **17**, 229–250.

James, R. and Ferris, F. G. (2004) Evidence for microbial-mediated iron oxidation at a neutrophilic groundwater spring. *Chem. Geol.* **212**, 301–311.

Kaczorek, D. and Sommer, M. (2003) Micromorphology, chemistry and mineralogy of bog iron ores from Poland. *Catena* **54**, 393–402.

Kamber, B. S., Bolhar, R. and Webb, G. E. (2004) Geochemistry of late Archean stromatolites from Zimbabwe: evidence for microbial life in restricted epicontinental seas. *Precambrian Res.* **132**, 379–399.

Kasama, T. and Murakami, T. (2001) The effect of microorganisms on Fe precipitation rates at neutral pH. *Chem. Geol.* **180**, 117–128.

Kennedy, C. B., Scott, S. D. and Ferris, F. G. (2003) Characterization of bacteriogenic iron oxide deposits from Axial Volcano, Juan de Fuca Ridge, Northeast Pacific Ocean. *Geomicrobiol. J.* **20**, 199–214.

Kennedy, C. B., Scott, S. D. and Ferris, F. G. (2004) Hydrothermal phase stabilization of 2-line ferrihydrite by bacteria. *Chem. Geol.* **212**, 269–277.

Konhauser, K. O., Hamade, T., Raiswell, R., Morris, R. C., Ferris, F. G., Southam, G. and Canfield, D. E. (2002) Could bacteria have formed the Precambrian banded iron formations? *Geology* **30**, 1079–1082.

Liu, X. D., Sun, L. G., Yin, X. B., Zhu, R. B., Xie, Z. Q. and Wang, Y. H. (2005) A preliminary study of elemental geochemistry and its potential application in Antarctic seal palaeoecology. *Geochem. J.* **39**, 47–59.

Lowenstam, H. A. (1981) Minerals formed by organisms. *Science* **211**, 1126–1131.

Lundgren, D. G. and Dean, W. (1979) Biogeochemistry of iron. *Biogeochemical Cycling of Mineral-Forming Elements* (Trudinger, P. A. and Swaine, D. J., eds.), 211–251, Elsevier Scientific Publishing Company, New York, U.S.A.

Mann, H., Tazaki, K., Fyfe, W. S. and Kerrich, R. (1992) Microbial accumulation of iron and manganese in different aquatic environments: an electron optical study. *Biominrealization: Processes of Iron and Manganese* (Skinner, H. C. W. and Fitzpatrick, R. W., eds.), 115–132, CatenaVerlag, Cremlingen, Germany.

McKay, D. S., Gibson, E. K., Jr., Thomas-Keprta, K. L., Vali, H., Romanek, C. S., Clemett, S. J., Chillier, X. D., Maechling, C. R. and Zare, R. N. (1996) Search for past life on Mars: possible relic biogenic activity in Martian meteorite ALH84001. *Science* **273**, 924–930.

Nealson, K. H. and Myers, C. R. (1990) Iron reduction by bacteria: a potential role in the genesis of banded iron formations. *Am. J. Sci.* **290A**, 35–45.

Petersen, K. (1997) Microbial life in deep granitic rock. *FEMS Microbiol. Rew.* **20**, 399–414.

Pontus, P. L. (1955) Geochemistry and radio activity of some Mn and Fe bog ores. *Geologiska Foereningens Foerhandlingar* **77**, 33–44.

Reid, R. P. and Browne, K. M. (1991) Intertidal stromatolites in a fring Holocene reef complex, Bahamass. *Geology* **19**, 15–18.

Schmitt, D., Taylor, H. E., Aiken, G. R., Rothd., A. and Frimmel, F. H. (2002) Influence of natural organic matter on the adsorption of metal ions onto clay minerals. *Environ. Sci. Technol.* **36**, 2932–2938.

Sobolev, D. and Roden, E. E. (2004) Characterization of a neutrophilic, chemolithoautotrophic Fe(II)-h-proteobacterium from freshwater wetland sediments. *Geomicrobiol. J.* **21**, 1–10.

Sun, L. G., Xie, Z. Q. and Shen, X. S. (2000) Ancient wood layer at Puda Bay in Zhujiajian Island, Zhejiang Province being discovered and its significance. *Ziran* **22**, 355–357 (in Chinese with English abstract).

Tazaki, K. (2000) Formation of banded iron-manganese structures by natural microbial communities. *Clays and Clay Minerals* **48**, 511–520.

Tazaki, K. (2005) Microbial formation of a halloysite-like mineral. *Clays and Clay Minerals* **53**(3), 224–233.

Tazaki, K., Ferris, F. G., Wiese, R. G. and Fyfe, W. S. (1992) Iron and graphite associated with fossil bacteria in chert. *Chem. Geol.* **95**(3–4), 313–325.

Tipping, E. and Hurley, M. A. (1992) Au unifying model of cation binding by humic hubstances. *Geochim. Cosmochim. Acta* **56**, 3627–3641.

Ueshima, M. and Tazaki, K. (2001) Possible role of microbial polysaccharides in nontronite formation. *Clays and Clay Minerals* **49**(4), 292–299.

Warren, L. A. and Haack, E. A. (2001) Biogeochemical controls on metal behavior in fresh water environments. *Earth-Sci. Rev.* **54**, 261–320.

Weber, J. H. (1988) Binding and transport of metals by humic materials. *Humic Substances and Their Role in the Environment* (Frimmel, F. H., ed.), 165–178, Wiley, New York, U.S.A.

Williams, K. H., Ntarlagiannis, D., Slater, L. D., Dohnalkova, A., Hubbard, S. S. and Banfield, J. F. (2005) Geophysical imaging of stimulated microbial biomineralization. *Environ. Sci. Technol.* **39**, 7592–7600.

Yuan, L. X., Sun, L. G., Wu, Z. J. and Zhang, S. Y. (2008) A 5600-year-old fossilized wood. *Journal of University of Science and Technology of China* **38**(1), 26–32 (in Chinese with English abstract).